

## Quad-Band Multilayer SIW Filter with High Selectivity and Controllable Bandwidths

Dinghong Jia<sup>1, \*</sup>, Jianqin Deng<sup>1</sup>, Yangping Zhao<sup>2</sup>, and Ke Wu<sup>2</sup>

**Abstract**—This work presents an approach for the design of a quad-band substrate integrated waveguide (SIW) bandpass filter based on multilayer process.  $TE_{101}/TE_{102}/TE_{103}/TE_{104}$  modes are used to characterize the four passbands, respectively. Firstly, the locations and band ratios of the passbands are chosen based on the effective width-length of the SIW resonator and its ratio. Then, vertical couplings of the modes and source-load are designed on the middle metal layers between the dielectric layers, which provides a relatively independent bandwidth tuning and high selectivity. To demonstrate the proposed design method, a quad-band SIW bandpass filter is fabricated and measured. Experimental results agree well with the simulated counterpart. The proposed quad-band SIW filter presents good selectivity and compact size.

### 1. INTRODUCTION

Due to its potential integration with other planar circuits, low insertion loss and easy fabrication, substrate integrated waveguide (SIW) becomes an effective solution for the design of microwave and millimeter-wave integrated circuits and systems [1]. Multi-band filters based on SIW have been developed for the modern communication systems advancing towards multi-mode characteristics and high integration [2–9]. The previous work mainly includes the designs of dual- and triple-band filters, which can be classified as three categories: loading etching apertures [2, 3], coupling matrix synthesis method [4, 5], and multi-mode dual-band SIW resonators [6–9]. Coupling matrix method is an effective way to design multi-band filters, but it is limited to the facts of the passbands adjacent to each other and large physical size. Multi-mode SIW resonators show the merit of compact size in the designing of multi-band filter. However, it is really hard to provide an effective method to control the bandwidth independently, since the modes always couple through the same window. In addition, to the knowledge of the authors, no quad-band SIW filter has been proposed in the literature because it is difficult to control so many modes.

In this work, a quad-band SIW filter based on  $TE_{101}/TE_{102}/TE_{103}/TE_{104}$  modes with high selectivity is proposed and demonstrated. Vertical couplings are adopted to generate the passbands and enable the source-load coupling. Relatively independent couplings are realized based on the field distribution of the selected modes, which provides a freely tuned bandwidth. Multi-mode characteristic and source-load coupling can produce transmission zeros near the passbands so as to improve the selectivity. The design procedure is also summarized. Finally, the proposed filter is experimentally validated.

### 2. FILTER DESIGN

Figure 1 illustrates the topology of the proposed quad-band multilayer SIW filter, which contains two dielectric layers and three metal layers. The selected resonant modes and source-load are vertically

---

*Received 18 February 2019, Accepted 15 April 2019, Scheduled 22 April 2019*

\* Corresponding author: Dinghong Jia (dinghongjia@gmail.com).

<sup>1</sup> Science and Technology on Electronic Test & Measurement Laboratory, The 41st Research Institute of CETC, Qingdao 266555, China. <sup>2</sup> Poly-Grames Research Center, Ecole Polytechnique, University of Montreal, QC H3T 1J4, Canada.

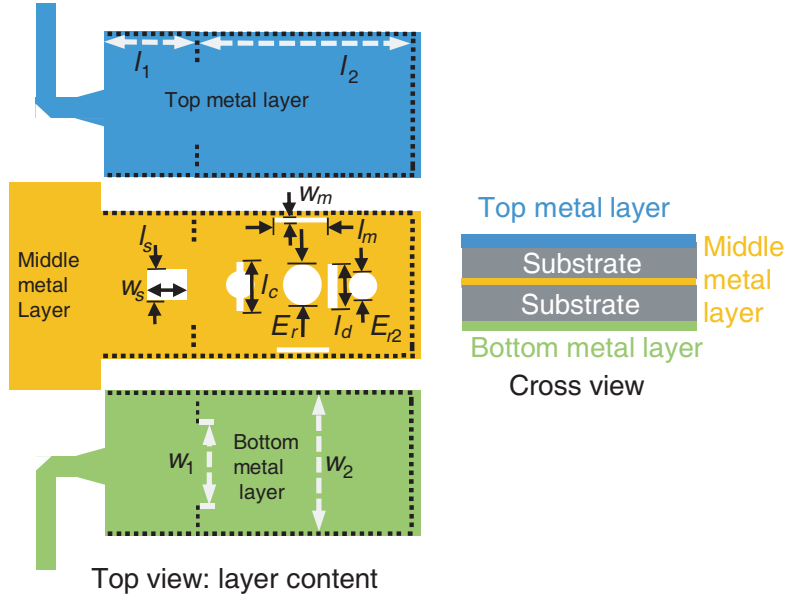


**Figure 1.** Structure of the proposed quad-band multilayer SIW filter.

coupled by apertures etched on the middle metallic interface. The four passbands are generated by  $TE_{10n}$  modes ( $n = 1, 2, 3,$  and  $4$ ), respectively. The filter is designed on a Rogers RT/Duroid 6002 substrate with thickness of 0.762 mm and loss tangent of 0.0012.

### 2.1. Resonator Design

In order to decide the center frequencies of the passbands and avoid the unwanted modes allocated in the frequency range of the four passbands, the dimensions of the SIW resonator should be accurately chosen. The resonant frequencies of  $TE_{m0n}$  mode can be calculated by the equations presented in [10] as

$$f_{TE_{m0n}} = \frac{c}{2\pi\sqrt{\epsilon_r}} \sqrt{\left(\frac{m\pi}{a}\right)^2 + \left(\frac{n\pi}{l}\right)^2} \quad (1)$$

where  $a$  and  $l$  are the effective width and length of the SIW resonator.  $\epsilon_r$  is the relative dielectric constant of the substrate, where  $m$  and  $n$  are the mode number of  $TE_{m0n}$  mode.

Define the mode ratio as:

$$r_{mn} = \frac{f_{TE_{m0n}}}{f_{TE_{101}}} \quad (2)$$

The ratio  $r_e$  of effective length  $l_{eff}$  and width  $w_{eff}$  of a SIW resonator is defined as:

$$r_e = \frac{l_{eff}}{w_{eff}} \quad (3)$$

Figure 2 presents the calculated results that are derived from Eqs. (1)–(3), considering all the modes near the passbands. The results are calculated under the conditions of variable  $l_{eff}$  with constant  $w_{eff} = 9$  mm. When  $r_e < 1.0$ , the first four resonant modes of the rectangle SIW resonator are intended to be  $TE_{101}$ ,  $TE_{201}$ ,  $TE_{102}$ , and  $TE_{202}$ . The maximum electric and magnetic fields of  $TE_{202}$  mode are completely overlapped with the maximum ones of  $TE_{201}$  and  $TE_{102}$ , which increases the difficulty to design a corresponding independent coupling of these modes.  $TE_{202}$  mode is therefore not suitable in our quad-band filter design. To avoid  $TE_{202}$ ,  $r_e$  should be larger than 1.6. Furthermore, additional structure or unbalanced feed is required to perturb the two degenerate modes  $TE_{201}$  and  $TE_{102}$ , which introduces new design difficulty [11, 12]. In summary,  $TE_{10n}$  ( $n = 1, 2, 3,$  and  $4$ ) modes are more

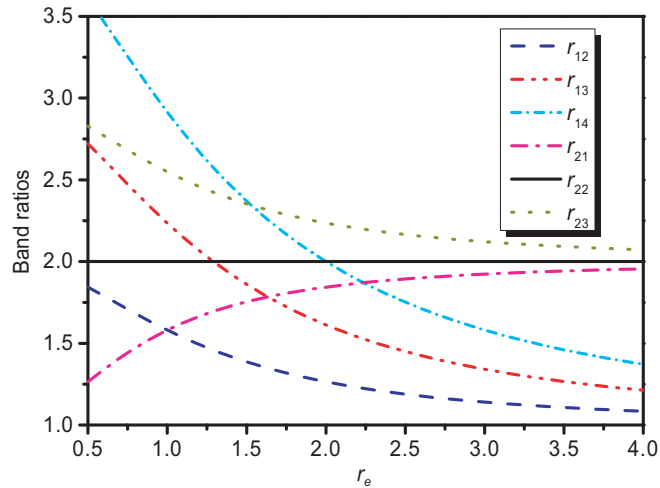


**Figure 2.** Band ratios  $r_{mn}$  tuning against  $r_e$ .

suitable to design the proposed quad-band filters, because the four modes can be generated by the same feeding, and they have different distributions of maximum electromagnetic fields as possible.

In order to ensure that the passbands are formed by  $TE_{10n}$  modes,  $r_e$  should be larger than 2.2. The first, second, and third higher-modes are  $TE_{102}$ ,  $TE_{103}$ , and  $TE_{104}$ , respectively. It can also be seen that  $r_{mn}$  decreases with the increase of  $r_e$ , which means that the frequency gap between different passbands of the filter becomes smaller. In other words, the center frequencies and its ratios of the four passbands of the proposed quad-band filter can be decided by the effective resonator width, length, and its ratio  $r_e$ .

## 2.2. Coupling Design

In a multi-mode multi-bands filter design, it is difficult to design independent couplings for different modes, which decides the bandwidths of the passbands. Thanks to the mode orthogonality of the resonant modes and the vertical coupled structure, it provides a relative independent coupling design. Fig. 3 illustrates the field distribution of the selected four modes and its coupling scheme through the middle metal layer.  $c_n$  and  $s_m$  ( $n = 1, 2, 3$  and  $m = 1, 2, 3, 4$ ) represent the etched three circular apertures and four slots, respectively.

Firstly, the magnetic and electric fields of fundamental mode  $TE_{101}$  couple through  $s_1$ ,  $s_2$ , and  $c_1$ , respectively. Secondly, the magnetic field of  $TE_{102}$  mode couples through  $c_1$  while the electric field couples through  $c_2$  and  $c_3$ . Thirdly, the electric field of  $TE_{103}$  mode couples through  $c_1$ ,  $c_2$ , and  $c_3$ , and the magnetic field couples through  $c_2$ ,  $c_3$ ,  $s_3$ , and  $s_4$ . Furthermore, the electric field of  $TE_{104}$  mode couples through  $s_4$ . Since the width of  $s_4$  is small, the electric coupling of  $TE_{104}$  is small enough to be ignored. Meanwhile, the magnetic field of  $TE_{104}$  mode couples through  $c_1$ ,  $c_2$ ,  $c_3$ , and  $s_3$ . It can be seen that the four modes couple through different apertures, which can provide a relative independent method to control the couplings. Finally, the source-load coupling is introduced to produce more transmission zeros so as to improve the selectivity of the passbands.

To validate the coupling scheme, Fig. 4 illustrates how the bandwidth is tuned by varying parameters of the etched apertures. Thanks to the multi-mode effects and source-load coupling, two transmission zeros are allocated at the low- and high-sides of each passband, respectively. In addition, one more transmission zero is generated at 11.5 GHz due to source-load coupling. As depicted in Fig. 4(a), the bandwidth of the first passband can be tuned by varying the widths of  $s_1$  and  $s_2$  while the other passbands almost keep constant. This phenomenon can be explained by the coupling scheme presented in Fig. 3. For higher-order modes  $TE_{103}$  and  $TE_{104}$ , the maximum magnetic fields are mainly generated at the middle of the resonator, that is to say  $s_1$  and  $s_2$  mainly enable the magnetic couplings of  $TE_{101}$  mode and produce small influence on the other couplings. Similarly, the bandwidth of the second passband can be tuned by varying the radii of  $c_2$  and  $c_3$  without producing any influence

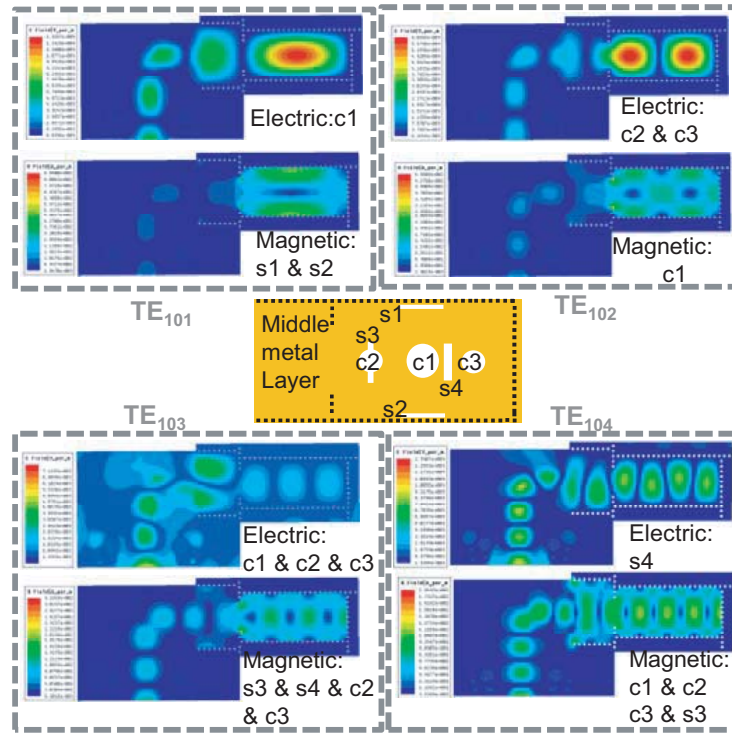
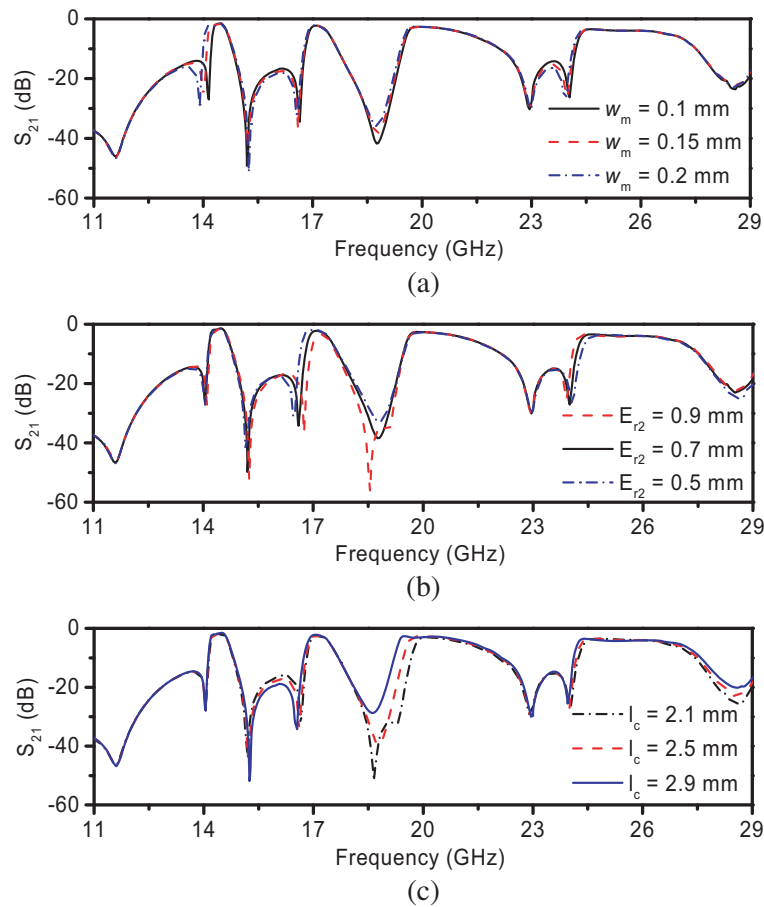
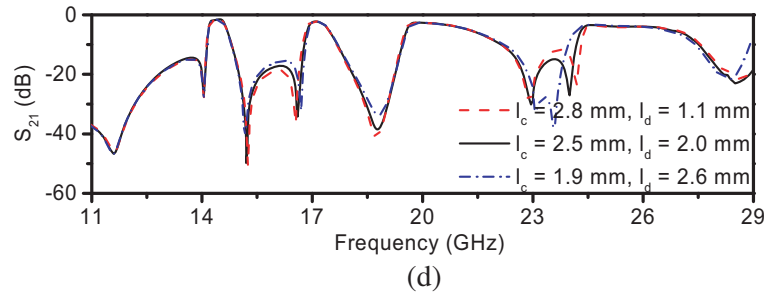


Figure 3. Field distribution and coupling scheme of the selected four modes.





**Figure 4.** Band tuning. (a) First passband. (b) Second passband. (c) Third passband. (d) Fourth passband.

on the first passband. Then, the bandwidth of the third passband can be tuned by varying the length of  $s_3$ . Meanwhile, the first two passbands present too small changes that can be ignored. Finally, the fourth passband can be changed by varying the length of  $s_3$ . To keep the third passband unchanged, the length of  $s_4$ , which only controls the magnetic couplings of TE<sub>103</sub> mode, needs to be tuned accordingly. By adopting the above-described methods, the bandwidths of the four passbands can be tuned independently. Additionally, the external factor  $Q_{ext}$  can also be used to determine the bandwidth, and it is mainly controlled by the source-to-resonator coupling. In this work, the required  $Q_{ext}$  can be achieved by tuning  $w_1$ .

The design procedure can be summarized as follows: 1) The center frequencies and band ratios of the passbands can be chosen based on the calculation presented in Eqs. (1)–(2) and Fig. 2; 2) The bandwidths of the four passbands can be tuned following the steps presented in Figs. 3 and 4; 3) The external quality of each passband can be realized by tuning the coupling widow width  $w_1$ . Following the proposed procedure, a quad-band SIW filter with independent bandwidth controlling and high selectivity can be achieved.

### 3. RESULTS AND DISCUSSION

To demonstrate the proposed filter, the multilayer SIW filter is designed with the center frequencies  $f_1 = 14.4$  GHz,  $f_2 = 17.0$  GHz,  $f_3 = 20.4$  GHz,  $f_4 = 25.5$  GHz, and 3-dB absolute bandwidths of 300, 520, 1640, and 2660 MHz. By following the above-described design procedure, the final dimensions are listed as below (unit: mm):  $l_1 = 5.2$ ,  $l_2 = 15.0$ ,  $w_m = 0.08$ ,  $l_m = 2.8$ ,  $l_c = 2.3$ ,  $w_c = 0.4$ ,  $l_d = 2.0$ ,  $w_d = 0.6$ ,  $E_r = 1.2$ ,  $E_{r2} = 0.75$ ,  $w_1 = 5.1$ ,  $w_2 = 6.8$ ,  $w_s = 2$ ,  $l_s = 2.6$ .

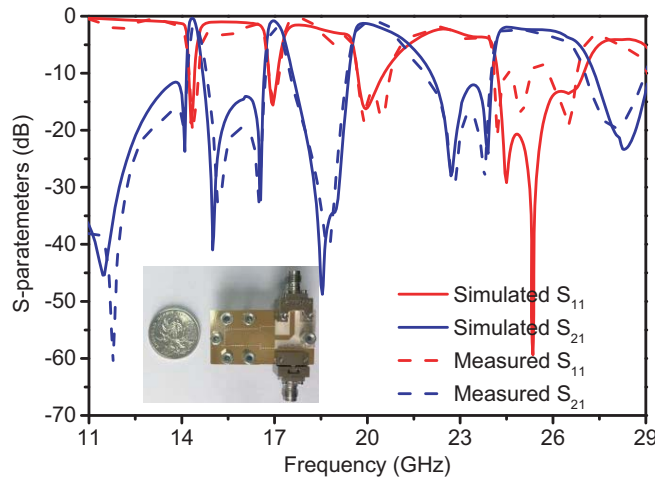


**Figure 5.** Photograph, simulated and measured results of the proposed filter.

Figure 5 shows that the measured  $S$ -parameters of the proposed filter agree very well with the simulation. A photograph of the fabricated circuit is also presented in the inset of Fig. 5. As can be seen, the selectivities of the passbands are significantly improved by the transmission zeros, which are mainly generated by the source-load coupling. The measured insertion losses of four passbands are 1.6, 2.2, 1.3, and 2.5 dB, respectively. In addition, the return losses of four passbands are all below 10 dB.

#### 4. CONCLUSION

An effective multilayer method is presented and validated for a quad-band SIW filter, and bandwidths of the passbands can be controlled independently. Additionally, the transmission zeros introduced by the source-load coupling and multi-mode effects are demonstrated to improve the selectivity. Compared with conventional horizontally coupled filters made of single layer, the proposed filter manifests the merits of independent bandwidths, high selectivity, and compact size.

#### ACKNOWLEDGMENT

This work was supported by the National Key R&D Program of China under Grant 2018YFF0109302 and 2018YFF0109702 and the Science and Technology on Electronic Test & Measurement Laboratory under Grant 9140C120102150C12055 and 6142001010101.

#### REFERENCES

1. Deslandes, D. and K. Wu, "Single-substrate integration technique of planar circuits and waveguide filters," *IEEE Trans. Microw. Theory Tech.*, Vol. 51, No. 2, 593–596, Feb. 2003.
2. Xu, S. S., K. X. Ma, F. Y. Meng, and K. S. Yeo, "Novel defected ground structure and two-side loading scheme for miniaturized dual-band SIW bandpass filter designs," *IEEE Microw. Wireless Compon. Lett.*, Vol. 25, No. 4, 217–219, Feb. 2015.
3. Lv, D.-D., L. Meng, and Z. Zou, "Miniaturized HMSIW dual-band filter based on CSRRs and microstrip open-stubs," *Progress In Electromagnetics Research Letters*, Vol. 77, 97–102, 2018.
4. Esmaili, M. and J. Bornemann, "Substrate integrated waveguide triple-passband dual-stopband filter using six cascaded singlets," *IEEE Microw. Wireless Compon. Lett.*, Vol. 24, No. 7, 439–441, Jul. 2014.
5. Chen, X. P., K. Wu, and Z. L. Li, "Dual-band and triple-band substrate integrated waveguide filters with Chebyshev and quasi-elliptic responses," *IEEE Trans. Microw. Theory Tech.*, Vol. 55, No. 12, 2569–2578, Dec. 2007.
6. Chen, B. J., T. M. Shen, and R. B. Wu, "Dual-band vertically stacked laminated waveguide filter design in LTCC technology," *IEEE Trans. Microw. Theory Tech.*, Vol. 57, No. 6, 1554–1562, Jun. 2009.
7. Shen, W., W. Y. Yin, and X. W. Sun, "Miniaturized dual-band substrate integrated waveguide filter with controllable bandwidths," *IEEE Microw. Wireless Compon. Lett.*, Vol. 21, No. 8, 418–420, Aug. 2011.
8. Wu, Y.-D., G. H. Li, W. Yang, and T. Mou, "A novel dual-band SIW filter with high selectivity," *Progress In Electromagnetics Research Letters*, Vol. 60, 81–88, 2016.
9. Zhou, K., C. X. Zhou, and W. Wu, "Substrate-integrated waveguide dual-mode dual-band bandpass filters with widely controllable bandwidth ratios," *IEEE Trans. Microw. Theory Tech.*, Vol. 65, No. 10, 3801–3812, Oct. 2017.
10. Pozar, D. M., *Microwave Engineering*, 3rd edition, Wiley, New York, 2005.
11. Chuang, C. C., H. H. Lin, and C. L. Wang, "Design of dual-mode SIW cavity filters," *2007 IEEE Region 10 Conference*, Taipei, Taiwan, Oct. 2007.
12. Almalkawi, M., L. Zhu, and V. Devabhaktuni, "Dual-mode substrate integrated waveguide (SIW) bandpass filters with an improved upper stopband performance," *2011 International Conference on Infrared, Millimeter, and Terahertz Waves*, Houston, TX, USA, Oct. 2011.